Supplementary Information

A framework for modelling electroactive biofilms performing direct electron transfer

Benjamin Korth[a], Luis F. M. Rosa[a], Falk Harnisch[a,*], Cristian Picioreanu[b]

[a] UFZ – Helmholtz-Centre for Environmental Research, Department of Environmental Microbiology, Permoserstrasse 15, 04318 Leipzig, Germany

[b] Department of Biotechnology, Faculty of Applied Sciences, Delft University of Technology, Julianalaan 67, 2628 BC Delft, The Netherlands.

Correspondance to:

* Falk Harnisch: falk.harnisch@ufz.de, Tel.: +49 341 235 – 1337, Fax: +49 341 235 – 1351

1 Model description

1.1 NAD^+/NADH

The Gibbs energy $\Delta G^{\theta'}_{f,NADH} - \Delta G^{\theta'}_{f,NAD+} = -E^{\theta'}_{NAD+/NADH}\, zF$ was estimated from the standard redox potential of the reduction reaction $NAD^+ + 2H^+ + 2e^- \rightarrow NADH + H^+$, $E^{\theta'}_{NAD^+/NADH} = -0.320\ V$ (vs. SHE) [1].

$$-NAD^+ - 2H^+ + NADH + H^+ = -E^{\theta'}_{NAD+/NADH}\, zF$$

$$(-NAD^+ + NADH) - H^+ = -E^{\theta'}_{NAD+/NADH}\, zF$$

$$(-NAD^+ + NADH) + 39.9\ \frac{kJ}{mol} = 0.320\ V \times 2 \times 96485.34\ \frac{C}{mol}$$

$$(-NAD^+ + NADH) = 21.85\ \frac{kJ}{mol}$$

Due to the strongly negative standard redox potential of the redox couple NAD^+/NADH the and according to the Nernst equation the concentration ratio $\frac{NAD^+}{NADH}$ has to be very huge in order to reach a more positive redox potential in respect to the substrate acetate ($E^{\theta'}_{acetate} = -0.280$ V vs. SHE) [2, 3]. In the beginning the concentration ratio $\frac{NAD^+}{NADH}$ is 1000:1.

1.2 Correction of the Gibbs energies

$\Delta G_{cat}^{\theta'}$ and $\Delta G_{an}^{\theta'}$ were corrected for the local reaction conditions (i.e. temperature, concentrations), by assuming standard conditions $C_{Ac-}^{\theta'} = C_{HCO3-}^{\theta'} = 1\ \text{mol L}^{-1}$ and $C_{H+}^{\theta'} = 10^{-7}\ \text{mol L}^{-1}$:

$$\Delta G_{cat} = \Delta G_{cat}^{\theta'} + RT\ln\left[\left(\frac{C_{HCO3-}}{C_{HCO3-}^{\theta'}}\right)^{2}\left(\frac{C_{H+}}{C_{H+}^{\theta'}}\right)^{5}\left(\frac{C_{NADH}}{C_{NAD+}}\right)^{4}\left(\frac{C_{Ac-}^{\theta'}}{C_{Ac-}}\right)\right]$$

$$\Delta G_{an} = \Delta G_{an}^{\theta'} + RT\ln\left[\left(\frac{C_{HCO3-}}{C_{HCO3-}^{\theta'}}\right)^{0.05}\left(\frac{C_{Ac-}^{\theta'}}{C_{Ac-}}\right)^{0.525}\left(\frac{C_{H+}^{\theta'}}{C_{H+}}\right)^{0.275}\right]$$

1.3 Cytochrome concentration

Cytochrome concentration is a critical parameter in modeling electroactive biofilms because there are still many uncertainties concerning amount, type and function of cytochromes in electrochemically-active biofilms. *Geobacteraceae* are known for producing more than 100 different types of cytochromes (with most cytochromes possessing more than one electron-binding haeme domain) [4] and different electron transfer mechanisms, *e.g.* $1H^+/\ 1e^-$ or $1H^+/\ 2e^-$ mechanisms. Furthermore, the amount of cytochromes may change with biofilm age and vary over the biofilm thickness [5, 6] and not all cytochromes within the cells are used for current production. Cytochromes are also used in metabolic pathways and there are indications for charge storage function within the biofilm [7]. For simplicity reasons we preferred to include in this model only one species of a c-type cytochrome possessing only one haeme and therefore only mid-point potential, and transferring one electron per molecule at a time, as cellular redox centre. Furthermore, all cytochromes are used for current production. As a first approach we used values based on fluorescence measurements in Esteve-Núñez *et al.* [8] which fits quite good with the value derived from the iterative approach (Section 3.1). The calculations were conducted with an electron storage capacity of $1.6\times10^{-17}\ \frac{\text{mol}}{\text{cell}}$ derived from [8] and a cell size of 1 µm length and a diameter of 0.3 µm.

$$V_{cell} = \pi \times r^2 \times l = \pi \times (0.15\ \mu m)^2 \times 1\ \mu m = 0.07\ \frac{\mu m^3}{\text{cell}}$$

$$C_{R/RH} = \frac{V_{cell}}{C_{haeme}} = \frac{0.07\ \frac{\mu m^3}{\text{cell}}}{1.6\times10^{-17}\ \frac{\text{mol}}{\text{cell}}} = 229\ \frac{\text{mol}}{m^3}$$

1.4 Considerations on microbial electron transfer and thermodynamics

The main difference between the Nernst-Monod and the Butler-Volmer approach is the assumption of thermodynamic equilibrium of the "gating" electron transfer reaction, i.e. the final electron transfer is not rate limiting and not affected by changes of the biofilm constitution (shrinking, growing, change in density). The Nernst-Monod equation requires no limitation caused by the charge

transfer between the redox active species and the electrode, whereas the terminal electron transfer can (but not has to) exclusively determine the reaction rate (current) in a Butler-Volmer approach. [9]. Since the biofilm growth (respectively current production) is not influenced by changes in heterogeneous electron transfer kinetics (Figure 2E-F, Figure SI 1) the Nernst-Monod approach would also be applicable. Nevertheless, the Nernst equation is a border case of the more general Butler-Volmer equation [9]. Because we wanted to establish a generally applicable biofilm model which would be also valid for more special cases, we used the Butler-Volmer approach. One cannot rule out the possibility that according to biofilm growth, pH changes etc. the "gating" electron transfer becomes rate limiting.

Furthermore, the Nernst-Monod equation [10] assumes that the whole potential difference between electron donor (*i.e.* acetate) and electron acceptor (*i.e.* anode) is used to gain energy by catabolic reactions and therefore regulates the substrate uptake. This is not the case for electroactive microbial biofilms, as the potential (*i.e.* energetic) difference between outer-membrane cytochromes and anode cannot be used by the bacteria to harvest energy. This energy difference is mostly used to overcome the overpotentials at the anode and would probably be converted into heat. Furthermore the potential difference between outer-membrane cytochromes and anode is much higher ($E_{cytochromes}$ = -0.136 V and E_{anode} = 0.4 V) than between the substrate acetate and the cytochromes ($E_{acetate}$ = -0.280 V and $E_{cytochromes}$ = -0.136 V). Therefore, using the Nernst-Monod approach would result in a too high energy gain and subsequently a much faster microbial growth than experimentally observed. Therefore in the proposed model the energy gain by microbial catabolism was simplified into one reaction, *i.e.* the electron transfer from acetate to NADH which was modeled using a double-Monod approach. The following electron transfer reactions are not used to gain energy and thus only serve to transfer electrons to the terminal acceptor (the anode).

Notably, the Butler-Volmer equation *per se* predicts no maximum electron transfer rate for the cytochromes. However, the rate of the electrochemical reaction will not increase (exponentially) because other coupled processes, like the substrate oxidation, will limit the growth and subsequently the electron transfer.

2 Chemical reactions

2.1 Chemical equilibria

Several acid-base equilibria exist within the biofilm and bulk electrolyte, and are mathematically described by using rate expressions (eq. (1)-(4)). The bulk liquid of the anodic compartment is considered as ideally mixed so that the ion concentration $C_{B,y}$ (subscript y represents the following ions: H+, OH-, AcH, Ac-, CO_2, HCO3-, H2PO4-, HPO4-2, Na+, Cl-) in the bulk liquid are uniform. The initial concentrations in the bulk liquid are derived from a system of algebraic equations formed with the chemical equilibria conditions (eq. (5)-(11)), electroneutrality (eq. (12)) condition and the set total concentrations of acetate $C_{0,Ac^-,T}$, phosphate $C_{0,H2PO4^-,T}$, and carbonate species $C_{0,CO2,T}$, which are assumed to be dissolved in the aqueous phase forming equilibria with their respective ionic species. Water dissociation allowing the calculation of the pH-value considers all present acid-base equilibria.

$$H_2O \rightleftarrows OH^- + H^+ \qquad r_{d,OH-} = k_W\left(1 - \frac{C_{H+}C_{OH-}}{K_W}\right) \tag{1}$$

$$CO_2 + H_2O \rightleftarrows HCO_3^- + H^+ \qquad r_{d,HCO3-} = k_{CO2}\left(C_{CO2} - \frac{C_{H+}C_{HCO3-}}{K_{CO2}}\right) \tag{2}$$

$$AcH \rightleftarrows Ac^- + H^+ \qquad r_{d,Ac-} = k_{AcH}\left(C_{AcH} - \frac{C_{H+}C_{Ac-}}{K_{d,AcH}}\right) \tag{3}$$

$$H_2PO_4^- \rightleftarrows HPO_4^{2-} + H^+ \qquad r_{d,H2PO4-} = k_{H2PO4-}\left(C_{H2PO4-} - \frac{C_{H+}C_{HPO4-2}}{K_{d,H2PO4-}}\right) \tag{4}$$

$$C_{0,CO2} = \frac{C_{0,CO2,T}C_{0,H+}}{\left(\frac{C_{0,H+}}{K_{d,CO2}} + 1\right)K_{d,CO2}} \tag{5}$$

$$C_{0,HCO3-} = \frac{C_{0,CO2,T}}{\left(\frac{C_{0,H+}}{K_{d,CO2}} + 1\right)} \tag{6}$$

$$C_{0,AcH} = \frac{C_{0,Ac-,T}C_{0,H+}}{\left(\frac{C_{0,H+}}{K_{d,AcH}} + 1\right)K_{d,AcH}} \tag{7}$$

$$C_{0,Ac-} = \frac{C_{0,Ac-,T}}{\left(\frac{C_{0,H+}}{K_{d,AcH}} + 1\right)} \tag{8}$$

$$C_{0,H2PO4-} = \frac{C_{0,H2PO4-,T}K_{d,H2PO4-}}{C_{0,H+} + K_{d,H2PO4-}} \tag{9}$$

$$C_{0,HPO4-2} = \frac{C_{0,H2PO4-,T}C_{0,H+}}{C_{0,H+} + K_{d,H2PO4-}} \tag{10}$$

$$C_{0,OH-} = \frac{K_{d,H2O}}{C_{0,H+}} \tag{11}$$

$$C_{0,Na+} = C_{0,OH-} + C_{0,HCO3-} + C_{0,Ac-} + C_{0,Cl-} + C_{0,H_2PO4-} + 2C_{0,HPO4-2} - C_{0,H+} \tag{12}$$

where K_W, $K_{d,CO2}$, $K_{d,AcH}$, $K_{d,H2PO4-}$ are equilibrium constants and k_W, k_{CO2}, k_{AcH}, k_{HPO4-2} are rate constants set at arbitrarily large values.

2.2 Dissolved chemical species in the biofilm

Dissolved chemical species exist in the biofilm, each with a concentration $c_{F,y}$, which are in contrast to the solute concentrations in the bulk liquid characterized by spatial concentration gradients. The initial concentrations in the biofilm are equal with those in bulk liquid $c_{B,y}(t=0)$. The Nernst-Planck equation with diffusion and ion migration, coupled with the electroneutrality condition, governs the transport and reaction of ions and neutral molecules in the biofilm:

$$\frac{\partial C_{F,i}}{\partial t} = \frac{\partial}{\partial x}\left(D_{F,i}\frac{\partial C_{F,i}}{\partial x} + z_i F \frac{D_{F,i}}{RT} C_{F,i}\frac{\partial \phi_L}{\partial x}\right) + r_{F,i} \qquad \sum_y z_y C_{F,y} = 0 \tag{13}$$

where z_y is the charge of the ion, $D_{F,y}$ is the diffusion coefficient in the biofilm (assumed for all species 50% of that in water, D_y), F is the Faraday constant and T is the temperature. Net component rates $r_{F,y}$ include biological ($r_{bio,y}$, $r_{m,y}$), chemical ($r_{d,y}$) and electrochemical ($r_{e,y}$) reactions calculated with local concentrations $C_{F,y}(x,t)$:

$$r_{F,Ac^-} = r_{bio,Ac^-} + r_{d,Ac^-} \tag{14}$$

$$r_{F,AcH} = -r_{d,Ac^-} \tag{15}$$

$$r_{F,HCO3^-} = r_{bio,HCO3^-} + r_{d,HCO3^-} \tag{16}$$

$$r_{F,CO2} = -r_{d,HCO3^-} \tag{17}$$

$$r_{F,HPO4^{2-}} = r_{d,HPO4^{2-}} \tag{18}$$

$$r_{F,H2PO4^-} = -r_{d,H2PO4^-} \tag{19}$$

$$r_{F,OH^-} = r_{d,OH^-} \tag{20}$$

$$r_{F,Na^+} = r_{F,Cl^-} = 0 \tag{21}$$

$$r_{F,H^+} = r_{bio,H^+} + r_{d,OH^-} + r_{d,HCO3^-} + r_{d,Ac^-} + r_{d,HPO4^{2-}} - r_{m,H^+} - r_{e,H^+} \tag{22}$$

The boundary conditions at the biofilm surface are: all concentrations equal with the bulk liquid concentrations $C_{F,y}(x = L_F, t) = C_{B,y}(t)$, an arbitrary reference potential $\phi_L(x = L_F, t) = 0$ and there is only ionic conductivity between the biofilm and the bulk liquid. Since no dissolved chemical species react at the electrode surface, zero-flux for all species and insulation for the aqueous potential are the boundary conditions applied at $x = 0$.

2.3 Dissolved chemical species in the bulk electrolyte

Concentrations of dissolved species, y, in the bulk liquid, $C_{B,y}(t)$, change in time due to charge balancing ion transfer, biofilm processes as well as the addition of new substrate, i.e. batch or repeated batch operation. Thus, the balance equations in the bulk liquid (V_B) includes contributions from reactions in the bulk liquid (acid-base, $r_{B,y}$), the ion flux exchanged with the biofilm ($J_{F,y}$) through the area of the biofilm exposed to the bulk (here considered equal with the electrode area, A_A), the flux through the membrane ($J_{M,y}$) with the membrane surface area (A_M) and, possibly, new medium additions or substitutions (the latter is not shown in equation (23)) :

$$\frac{dC_{B,y}}{dt} = r_{B,y} + J_{F,y}\frac{A_A}{V_B} + J_{M,y}\frac{A_M}{V_B} \tag{23}$$

The coupling between bulk liquid and biofilm is therefore bidirectional: The concentration $C_{B,y}$ of a chemical species in the bulk is the boundary condition for its concentration, $C_{F,y}$, in the biofilm. Thus, the flux between these two compartments:

$$J_{F,y} = \left(D_{F,y}\frac{\partial C_{F,y}}{\partial x} + z_y F \frac{D_{F,y}}{RT} C_{F,y}\frac{\partial E_L}{\partial x}\right)_{x=L_F} \tag{24}$$

contributes to the change of bulk concentration. $E_L(x,t)$ is the potential in the aqueous phase of the biofilm. The fluxes of cations (y = H+, Na+) through the membrane ($J_{M,y}$) arise from diffusion and ion migration through the membrane[1]:

$$J_{M,y} = \frac{D_{M,y}}{L_M}\left(C_{B,y} - C_{C,y}\right) + \frac{F}{RT}\frac{D_{M,y}}{L_M}\frac{C_{B,y} + C_{C,y}}{2}\frac{F\sum_j z_j C_{B,j}}{\varepsilon_0 \varepsilon_M} L_M^2 \qquad (25)$$

where $D_{M,y}$ is the diffusion coefficient through the membrane, L_M is the membrane thickness, $C_{C,y}$ is the ion concentration in the cathodic solution which is initially identical with the concentration in the anode compartment, and ε_M is the relative dielectric coefficient of the membrane and ε_0 the vacuum permittivity.

3 Results

3.1 Macroscopic level: Biofilm growth and current production

3.1.1 Used parameters

All used parameters derived from Table 1 except the values listed in Table S1.

Table S1 Specific parameters used to represent the biofilm growth experiment from Bond & Lovley [11]:

Parameter description	Symbol	Value	Units	Source
Bulk liquid				
Bulk liquid volume	V_B	225	mL	[11]
Initial concentrations in bulk liquid and biofilm				
- total initial acetate and acetate Additions	$C_{0,Ac^-,T}$	1.0	mol / m^3	[11]
- total bicarbonate	$C_{0,HCO3^-}$	23.8	mol / m^3	[11]
- total phosphate	$C_{0,H2PO4^-,T}$	5.0	mol / m^3	[11]
- H^+	C_{0,H^+}	$10^{-6.8}$	mol / L	[11]
Electrochemical kinetics and electrical properties				
Electrode potential	E_A	0.4	V (SHE)	[11]
Biofilm properties				
Initial Biofilm thickness	L_{F0}	1	µm	Chosen
Biofilm area and electrode area	A_A	61.2	cm^2	[11]
Concentration oxidized/reduced redox centres	$C_{R/RH}$	300	mol / m^3	Chosen
Biofilm / electrode electron transfer rate coefficient	k_c^0	0.03	1 / s	[12]

3.1.2 *Modeling of electroactive microbial anodes with different values for electrochemical parameters*

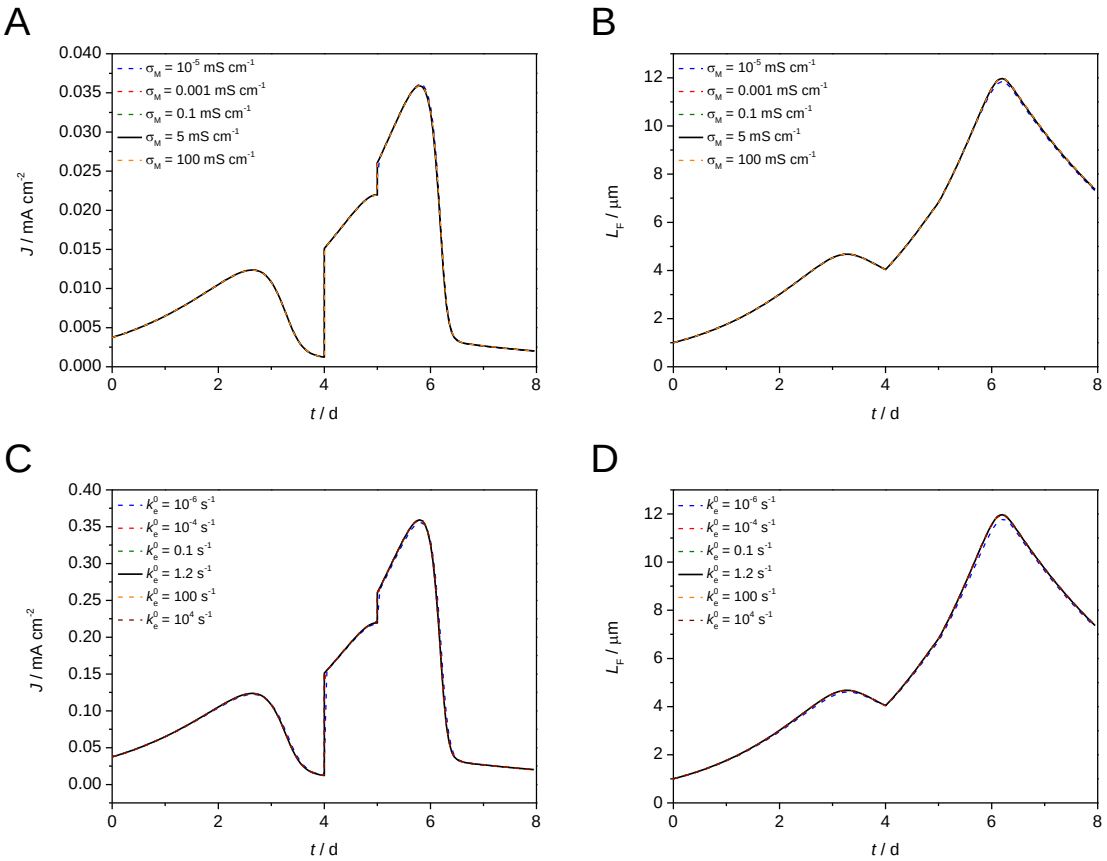

Figure S1 Simulation results of electroactive microbial anodes based on *direct electron transfer*. **(A-B)** Resulting current density and biofilm thickness with several values for conductivity within the biofilm (σ_M). **(C-D)** Resulting current density and biofilm thickness with several values for the standard homogeneous electron transfer rate (k_e^0 , cell/biofilm matrix). The used model parameters are listed in Table 1 and Table S1.

3.1.3 *Modeling electroactive microbial anodes with different values for metabolic parameters*

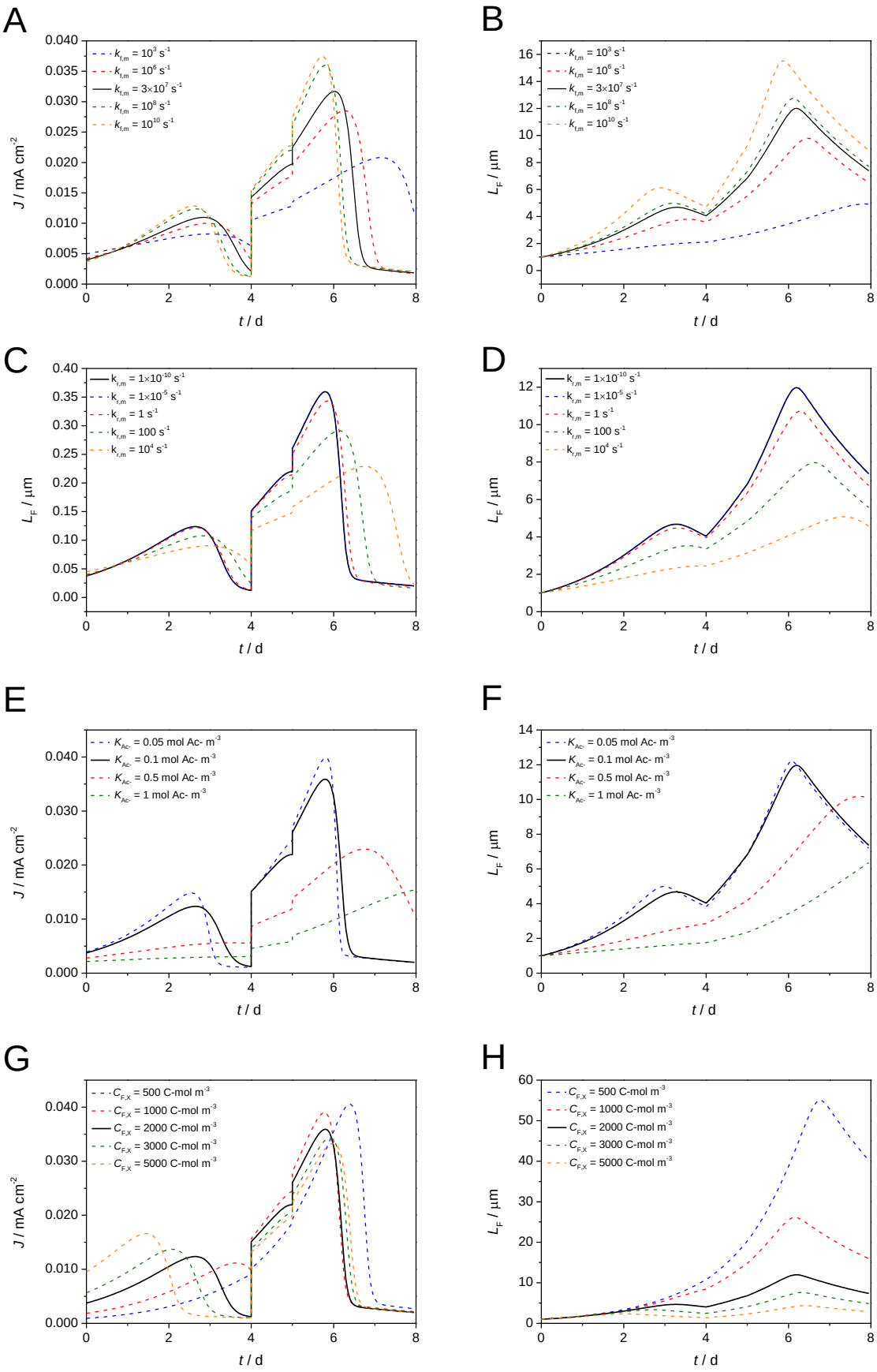

Figure S2 **(A-B)** Resulting current density and biofilm thickness with several values for the forward rate for the intracellular electron transfer rate from NADH to oxidized cytochromes ($k_{f,m}$). **(C-D)** Resulting current density and biofilm thickness with several values for the reverse rate for the intracellular electron transfer rate from reduced cytochromes to NADH ($k_{r,m}$). **(E-F)** Resulting current density and biofilm thickness with several values for the half-saturation coefficient for acetate (K_{Ac-}). **(G-H)** Resulting current density and biofilm thickness with several values for biomass concentration ($C_{F,X}$).The used model parameters are listed in Table 1 and Table S1.

3.2 Spatial resolution on the biofilm level

3.2.1 Used parameters

All used parameters are derived from Table 1 except the values listed in Table S2.

Table S2 Specific parameters used to represent the pH measurements of Franks *et al.* [13]:

Parameter description	**Symbol**	**Value**	**Units**	**Source**
Bulk liquid				
Bulk liquid volume	V_B	500	mL	[13]
Initial concentrations in bulk liquid and biofilm				
- total acetate	$C_{0,Ac-,T}$	10.0	mol / m^3	[13]
- total bicarbonate	$C_{0,HCO3-}$	1.0 - 50.0	mol / m^3	Chosen
- H^+	$C_{0,H+}$	10^{-7}	mol / L	[13]
Electrochemical kinetics and electrical properties				
Electrode potential	E_A	0.3	V (Ag/AgCl)	[13]
Biofilm properties				
Initial Biofilm thickness	L_{F0}	0.1	µm	Chosen
Biofilm area and electrode area	A_A	0.81	cm^2	[13]
Concentration oxidized/reduced redox centres	$C_{R/RH}$	300	mol / m^3	Chosen
Biofilm / electrode electron transfer rate coefficient	k_c^0	0.03	1 / s	[12]

Due the fact that the experimental buffer compositions are not mentioned in [13], buffer compositions of the cited article [14] are used in the model. In line with the experimental conditions the bulk concentrations were kept constant.

3.2.2 Redox profiles in electroactive biofilms modeling Franks et al. [13]

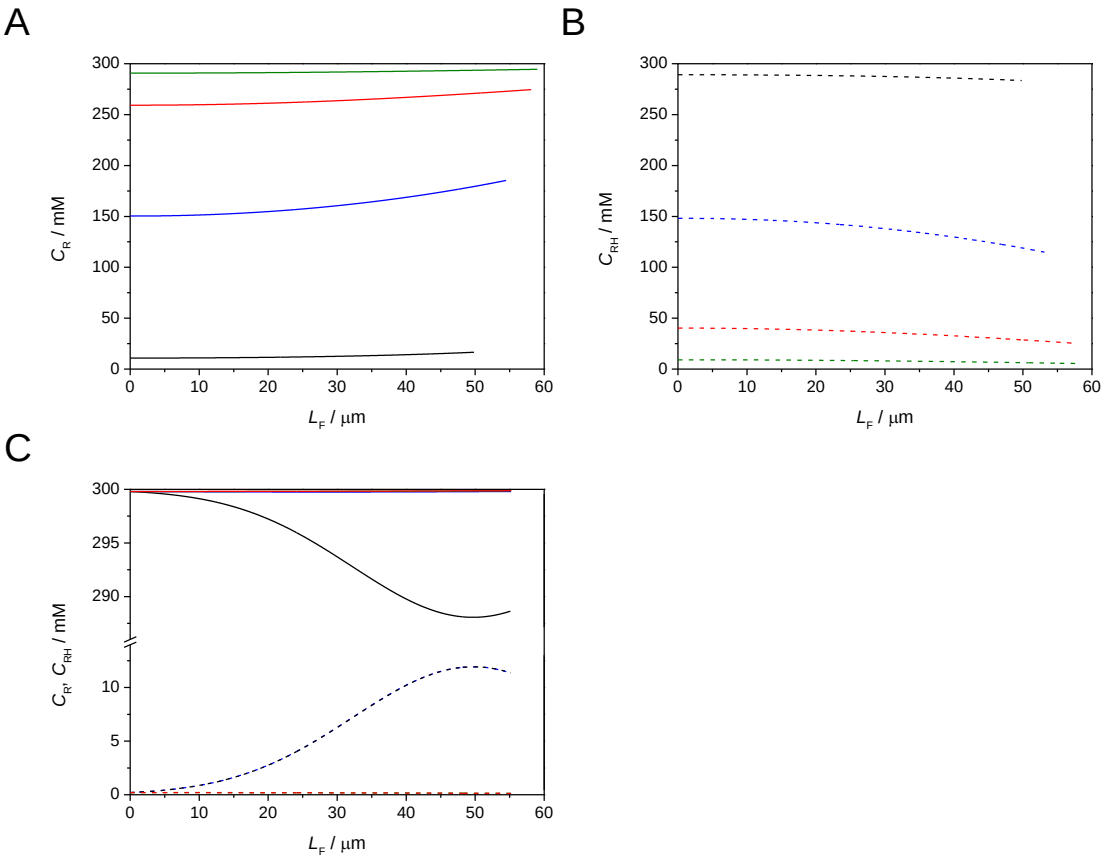

Figure S3 **(A-B)** Profiles of oxidized cytochromes (C_R) and reduced cytochromes (C_{RH}) in biofilms with a constant attenuation factor for diffusion ($\varepsilon_D = 0.5$), a constant bicarbonate buffer composition ($C_{0,HCO3-} = 5$ mM) and different values for the heterogeneous electron transfer rate (k_c^0). 10^{-7} s^{-1} (black), 10^{-6} s^{-1} (blue), 10^{-5} s^{-1} (red), 10^{-4} s^{-1} (green). **(C)** Redox profile (profiles of oxidized (C_R, solid lines) and reduced cytochromes (C_{RH}, dashed lines)) in biofilms with a constant attenuation factor for diffusion ($\varepsilon_D = 0.5$), a constant bicarbonate buffer composition ($C_{0,HCO3-} = 5$ mM) and different values for biofilm matrix conductivity (σ_M). 0.0005 mS cm^{-2} (black), 0.005 mS cm^{-2} (blue), 0.05 mS cm^{-2} (green), 5 mS cm^{-2} (red). Model parameters are listed in Table 1 and Table S2.

3.2.3 Redox profiles in electroactive biofilms modeling Bond & Lovley [11]

Modeling Bond & Lovley [11] with parameters listed in Table 1 and Table S1. Several values for the heterogeneous electron transfer rate were tested. The concentration of oxidized and reduced cytochromes are calculated for the time 5.8 d while the maximum current density peak and the maximum biofilm thickness were recorded.

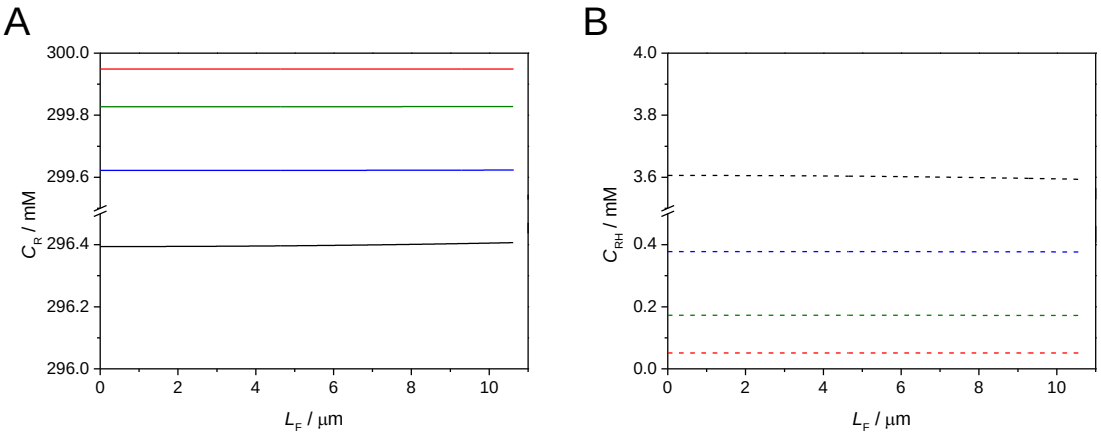

Figure S4 Redox profiles (concentration of oxidized/reduced cytochromes, $C_{R/RH}$) in the biofilm with several values for the heterogeneous electron transfer rate (k_c^0) for the respective simulation of the Bond & Lovley experiment (see Figure 1A). 0.001 s^{-1} (black), 0.03 s^{-1} (blue), 0.1 s^{-1} (green), 1 s^{-1} (red) **(A)** Oxidized cytochromes (C_R). **(B)** Reduced cytochromes (C_{RH}). Model parameters are listed in Table 1 and Table S1.

3.3 Biofilm electron transfer

3.3.1 *Non-turnover cyclic voltammetry modeling Jana et al.* [15]

3.3.1.1 *Used parameters*

All used parameters are derived from Table 1 except the values listed in Table S3.

Table S3 Specific parameters used to represent the non-turnover CV experiments of Jana *et al.* [15]:

Parameter description	Symbol	Value	Units	Source
Bulk liquid				
Bulk liquid volume	V_B	100	mL	[15]
Initial concentrations in bulk liquid and biofilm				
- total acetate	$C_{0,Ac^-,T}$	0	mol / m^3	[15]
- total bicarbonate	$C_{0,HCO3^-}$	29.7	mol / m^3	[15]
- total phosphate	$C_{0,H2PO4^-,T}$	4.2	mol / m^3	[15]
- H^+	C_{0,H^+}	$10^{-7.35}$	mol / L	[15]
Electrochemical kinetics and electrical properties				

Electrode potential	E_A	-0.7 – 0.3	V (SHE)	[15]
Scan rate	v	5 – 60	mV / s	[15]
Biofilm properties				
Initial Biofilm thickness	L_{F0}	5, 50	µm	[15]
Biofilm area and electrode area	A_A	1.77	cm^2	[15]
Concentration oxidized/reduced redox centres	$C_{R/RH}$	3	mol / m^3	Chosen
Biofilm / electrode electron transfer rate coefficient	k_c^0	1.2	1 / s	Chosen

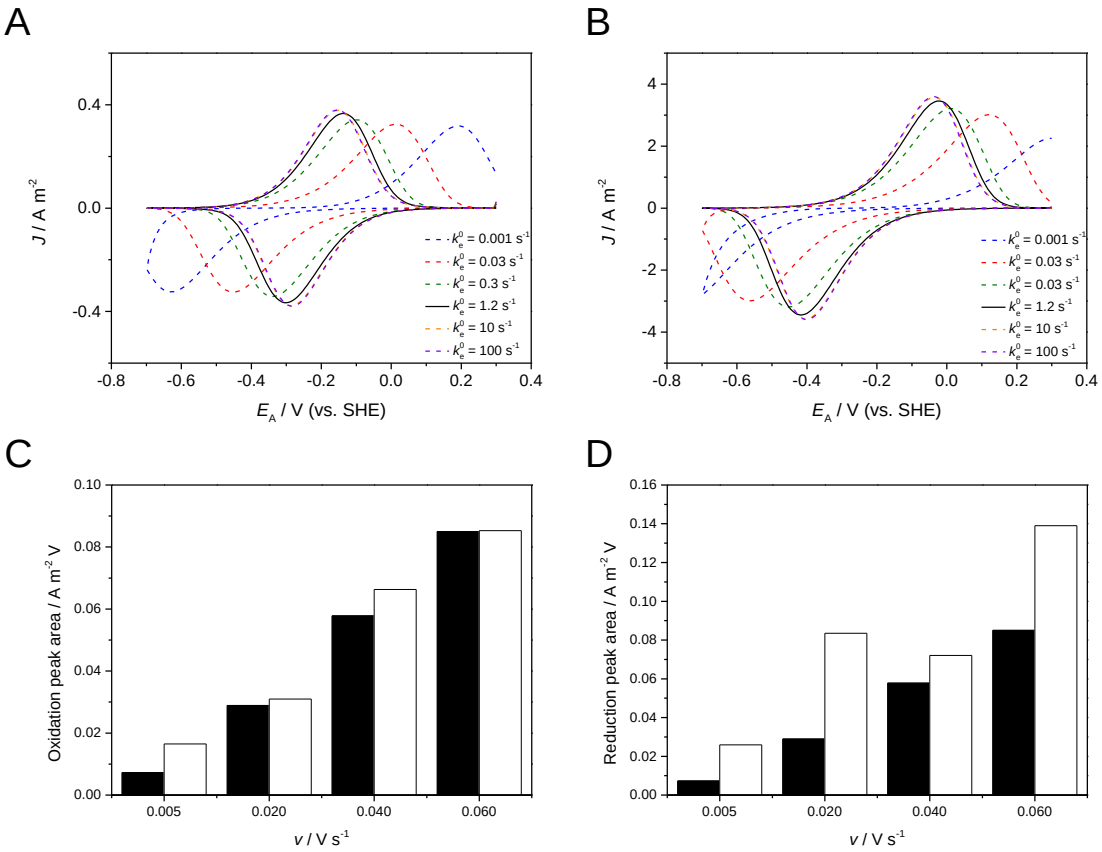

Figure S5 Modeled cyclic voltammograms with several values for the homogeneous electron transfer rate (k_e^0) in a **(A)** 5 µm and **(B)** 50 µm biofilm. Peak area comparison between modeled (black bars) and real (white bars) data from *Jana et al.* in 5 µm biofilms. **(C)** Areas of oxidative scans, and **(D)** areas of reductive scans. Model parameters are listed in Table 1 and Table S3.

3.3.2 Turnover cyclic voltammetry modeling Fricke *et al. [16]*

3.3.2.1 *Used parameters*

All used parameters are derived from Table 1 except the values listed in Table S4.

Table S4 Specific parameters used to represent the turnover CV experiments of Fricke *et al.* [16]:

Parameter description	**Symbol**	**Value**	**Units**	**Source**
Bulk liquid				
Bulk liquid volume	V_B	225	mL	[11]
Initial concentrations in bulk liquid and biofilm				
- total initial acetate	$C_{0,Ac^-,T}$	3.0	mol / m^3	Adapted from [16]
- total bicarbonate	$C_{0,HCO3^-}$	23.8	mol / m^3	[11]
- total phosphate	$C_{0,H2PO4^-,T}$	5.0	mol / m^3	[11]
- H^+	C_{0,H^+}	$10^{-6.8}$	mol / L	[11]
Electrochemical kinetics and electrical properties				
Electrode potential	E_A	-0.7 – 0.3	V (Ag/AgCl)	[16]
Scan rate	v	5	mV / s	[16]
Biofilm properties				
Initial Biofilm thickness	L_{F0}	27.5	µm	Chosen
Biofilm area and electrode area	A_A	61.2	cm^2	[11]
Concentration oxidized/reduced redox centres	$C_{R/RH}$	1	mol / m^3	Chosen
Biofilm / electrode electron transfer rate coefficient	k_c^0	1.2	1 / s	Chosen

3.3.2.2 *Modeling electroactive biofilms with different values for initial biofilm thickness and biofilm matrix conductivity*

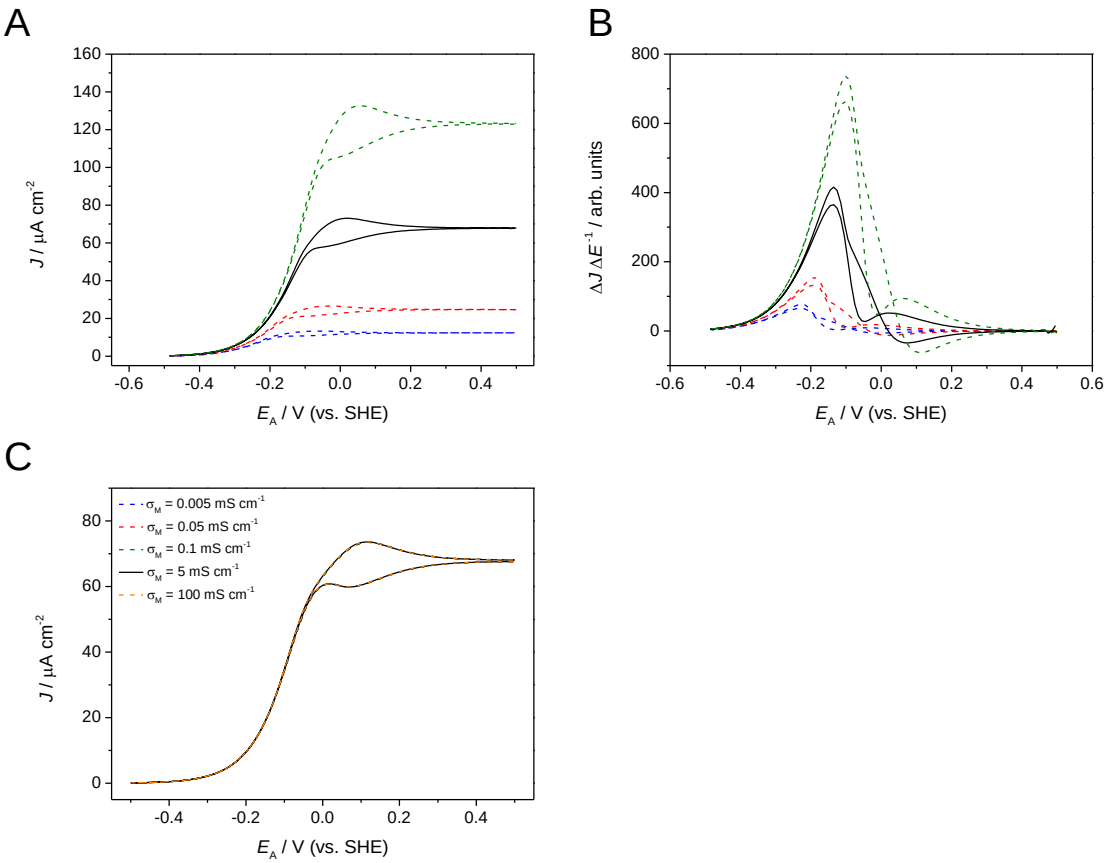

Figure S6 Simulation results of electroactive biofilms in cyclic voltammetry experiments under turnover conditions (v = 5 mV s^{-1}) modeling Fricke *et al.* [16]. **(A)** Resulting current density with several values for initial biofilm thickness (L_{F0}). 5 µm (blue dashed line), 10 µm (red dashed line), 27.5 µm (solid line), 50 µm (green dashed line).
(B) Corresponding 1st derivative of the resulted current. 5 µm (blue dashed line), 10 µm (red dashed line), 27.5 µm (solid line), 50 µm (green dashed line).
(C) Resulting current density with several values for biofilm matrix conductivity (σ_M). Model parameters are listed in Table 1 and Table S4.

3.3.2.3 *Modeling electroactive biofilms with different values for the substrate oxidation rate*

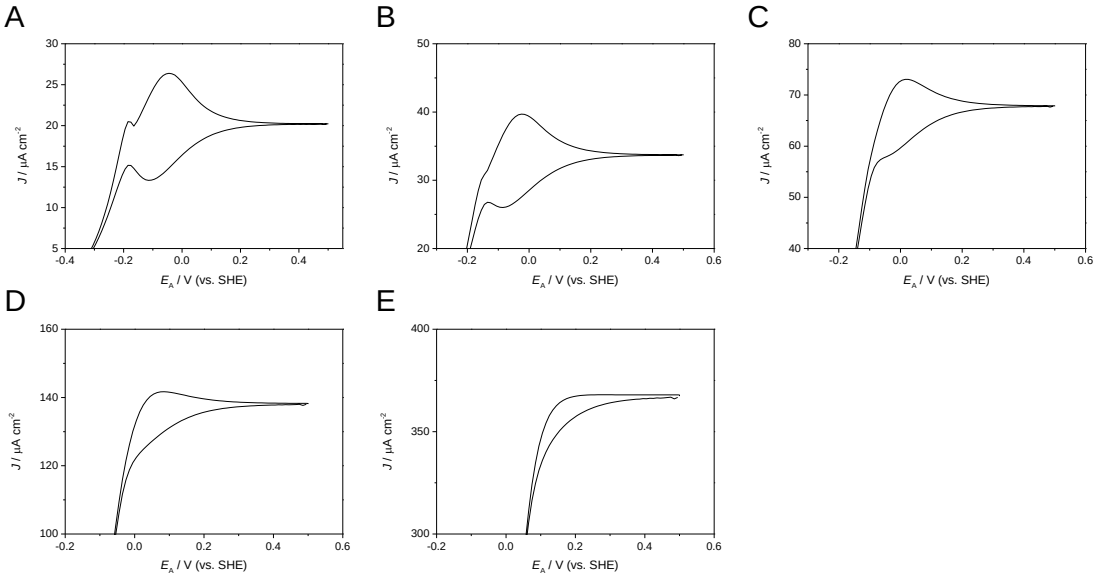

Figure S7 Section of simulation results of electroactive biofilms in cyclic voltammetry experiments under turnover conditions (v = 5 mV s^{-1}) modeling Fricke *et al.* [16]. The calculated substrate oxidation rate (q_{Ac^-}, Section 2.1.1) was artificial changed during the simulations to show the impact of the catabolic reaction to the second peak pair in the range of 0 V (vs. SHE). **(A)** $\frac{q_{Ac^-}}{3}$. **(B)** $\frac{q_{Ac^-}}{2}$. **(C)** q_{Ac^-}. **(D)** $2 \times q_{Ac^-}$. **(E)** $5 \times q_{Ac^-}$. Model parameters are listed in Table 1 and Table S4.

4 References

1. Burton, K., *Free energy data of biological interest.* Ergebnisse der Physiologie, 1957. **29**: p. 212-298.
2. Thauer, R.K., et al., *Energy conservation in chemotrophic anaerobic bacteria.* Bacteriol. Rev., 1977. **41**: p. 809.
3. Heijnen, J.J. and R. Kleerebezem, *Bioenergetics of Microbial Growth*, in *Encyclopedia of Industrial Biotechnology: Bioprocess, Bioseparation and Cell Technology*, M.C. Flickinger, Editor. 2010, John Wiley & Sons, Inc.
4. Methe, B.A., et al., *Genome of Geobacter sulfurreducens: metal reduction in subsurface environments.* Science, 2003. **302**(5652): p. 1967-9.
5. Inoue, K., et al., *Specific localization of the c-type cytochrome OmcZ at the anode surface in current-producing biofilms of Geobacter sulfurreducens.* Environ. Microbiol. Rep., 2011. **3**(2): p. 211-7.
6. Franks, A.E., R.H. Glaven, and D.R. Lovley, *Real-time spatial gene expression analysis within current-producing biofilms.* ChemSusChem, 2012. **5**(6): p. 1092-8.
7. Malvankar, N.S., et al., *Supercapacitors Based on c-Type Cytochromes Using Conductive Nanostructured Networks of Living Bacteria.* Chem. Phys. Chem., 2012. **13**(2): p. 463-468.
8. Esteve-Nunez, A., et al., *Fluorescent properties of c-type cytochromes reveal their potential role as an extracytoplasmic electron sink in Geobacter sulfurreducens.* Environ. Microbiol., 2008. **10**(2): p. 497-505.
9. Bard, A.J., G. Inzelt, and F. Scholz, *Electrochemical Dictionary*. 2nd ed. 2012: Springer.

10. Torres, C.I., B.E. Rittmann, and A.K. Marcus, *Conduction-based modeling of the biofilm anode of a microbial fuel cell.* Biotechnol. Bioeng., 2007. **98**(6): p. 1171-1182.
11. Bond, D.R. and D.R. Lovley, *Electricity production by Geobacter sulfurreducens attached to electrodes.* Appl. Environ. Microb., 2003. **69**(3): p. 1548-1555.
12. Ly, H.K., et al., *Unraveling the interfacial electron transfer dynamics of electroactive microbial biofilms using surface-enhanced Raman spectroscopy.* Chem. Sus. Chem., 2013. **6**: p. 487-92.
13. Franks, A.E., et al., *Novel strategy for three-dimensional real-time imaging of microbial fuel cell communities monitoring the inhibitory effects of proton accumulation within the anode biofilm.* Energ. Environ. Sci., 2009. **2**(1): p. 113-119.
14. Lovley, D.R. and E.J.P. Phillips, *Novel mode of microbial energy metabolism organic carbon oxidation coupled to dissimilatory reduction of iron.* Appl. Environ. Microb., 1988. **54**: p. 1472-1480.
15. Jana, P.S., et al., *Charge transport in films of Geobacter sulfurreducens on graphite electrodes as a function of film thickness.* Phys. Chem. Chem. Phys., 2014. **16**(19): p. 9039-46.
16. Fricke, K., F. Harnisch, and U. Schröder, *On the use of cyclic voltammetry for the study of anodic electron transfer in microbial fuel cells.* Energ. Environ. Sci., 2008. **1**: p. 144-147.